Supporting Information

Ordered Mesoporous Silica Microsphere for Supercritical Fluid Chromatography

Chunying Song[ab], Yi Qi[c], Chenyu Wang[c], Gaowa Jin[a], Shengfu Wang[c], Dongping Yu[c], Zhimou Guo[a*], Xinmiao Liang[a*]

Experimental section

Chemicals and materials: HPLC-grade methanol (MeOH), isopropyl alcohol (IPA), and n-hexane were purchased from J&K (Beijing, China). All analytes of Table S1 were obtained from Macklin (Shanghai, China) and dissolved in MeOH at a concentration of 1 mg/mL. The analytes of Table S6 were either purchased from different manufacturers. Their chemical structures and detailed information were listed in Table S6. Tetraethoxysilane (TEOS, 98%), 3-mercaptopropyltriethoxysilane and dodecylamine (DDA) were purchased from Sigma-Aldrich (St. Loius, MO, USA). Water was purified using a Milli-Q purification system (Billerica, MA, USA). Spherical silica (2.5 μm particle size, 100 Å pore size) was purchased from Fuji Silysia Chemical (Kasugai, Japan). High-purity grade carbon dioxide (99.99%) was purchased from Jiangxi East-China Special Gases Co., Ltd (Nanchang, China). The extract of Salvia miltiorrhiza Bunge was prepared in our laboratory. PIC column was supplied by Waters (Milford, MA, USA), with 150 mm ×4.6 mm I.D. and 5 μm particle size. NH2 (100 mm × 4.6 mm, 3.5μm), and Diol (100 mm × 4.6 mm, 3.5 μm) columns were from Acchrom (Beijing, China). The stainless-steel column tubes (100 mm × 4.6 mm, 100 mm × 3 mm, 50 mm × 4.6 mm) and sieve plate (0.5 μm) were purchased from IDEX (Northbrook, IL, USA).

Synthesis and column packing: OMS was synthesized according to previously reported method[1]. For 2.33 μm particle size, dodecylamine (7.2 mL) with a concentration of 40 mmol/L was added into a mixture containing 360 mL methanol and 150 mL water. After dodecylamine was well dissolved, 28.8 mL TEOS was added and the solution was vigorously stirred at 30 ℃ until the solution turned opaque. Then, the mixture was maintained under static condition for 24 h until the formed particles were

settled down to the flask bottom. After removing the liquid by centrifugation, the precipitates were washed with massive water and methanol. The products were dried at 80 ℃ for 24 h and calcined at 600 ℃ for 8 h. The prepared sample was designated as 2.33 μm OMS. For 1.10 μm OMS preparation, the only change is the concentration of dodecylamine was adjusted to 120 mmol/L. For chromatographic evaluations, 1.8 g 2.33 μm OMS was slurry-packed into a stainless-steel column (100 × 4.6 mm I.D.) under 60 MPa using methanol as slurry solvent and isopropyl alcohol as propulsion solvent. 1 g 1.10 μm OMS and 1 g OMS-SH were respectively slurry-packed into a stainless-steel column (50 × 4.6 mm I.D.) under 50 MPa using methanol as slurry solvent and isopropyl alcohol as propulsion solvent.

Instrument and characterization: SFC separation was performed on Agilent 1260 Infinity SFC Analytical System, which includes binary solvent delivery pump, autosampler, column manager, photodiode array detector, and back pressure regulator. Data acquisition and control of the equipment were carried out on the OpenLab CDS software. Van Deemter curves were tested on a Waters Corporation ACQUITY Ultra Performance Convergence Chromatography™ (UPC^2). It was equipped with a binary solvent delivery pump compatible with mobile phase flow rates up to 4 mL/min and pressures up to 414 bar, an autosampler (with a 10-μL loop), a column manager, an automatic back pressure regulator (ABPR), and a photodiode-array (PDA) detector. SEM images were obtained on FlexSEM 1000 II with 3.5 kV accelerating voltage and 10 nm probe distance. TEM images were obtained on FEI Talos F200s with 100 kV operating voltage. High resolution TEM photograph of 2.33 μm OMS was obtained from FEI Titan Themis ETEM G3 200 kV operating voltage. Nitrogen sorption experiments were performed on QuadraSorb evo surface area/pore size analyzer. Surface area and pore size distribution were calculated using Brunauer–Emmett–Teller (BET) and non-local density functional theory (NLDFT) method. Small-angle X-ray scattering (SAXS) patterns were obtained on Xeuss 2.0 (xenocs, France) with Cu Kα radiation beam (λ = 1.5418 Å) in the 2θ range of 0-8° at room temperature. When identifying tanshinone components, the SFC system was coupled to an Agilent 6540 Q-TOF spectrometry system equipped with an electrospray ionization interface. For

MS detection, the ESI† source was operated in positive ion mode to acquire MS/MS spectra. The collision energy was 40 eV and 20 eV, and the MS and MS/MS ranges of data acquisition were 100-1000 Da. MassHunter 10.0 software (Agilent) was used for data acquisition and to control the Q-TOF mass spectrometry system. X-ray photoelectron spectroscopy (XPS) measurements were performed under high vacuum conditions using a Physical Electronics PHI 5000 VersaProbe XPS spectrometer with monochromatic Al Kα radiation (1486.6 eV) equipped with a hemispherical energy analyzer. Vario EL III elemental analyzer was applied to obtain the elemental analysis results of modified OMS (OMS-SH). The mean diameters of OMS, OMS-SH and silica gel were examined by a laser particle size analyzer (Brookhaven, 90plus). The mean diameter of 1.10 μm OMS was tested by nanometer particle size potentiometer with higher precision (Malvern Panalytical Nano-ZS90).

Test conditions for Van Deemter curves and column efficiency: The BPR pressure was set to 2100 psi (≈145 bar), the mobile phases included A (supercritical fluid CO_2) and B (methanol). For 2.33 μm OMS (100 × 3 mm I.D.), the A/B = 85/15 (v/v), and the flow rate ranges from 0.2 to 4.0 mL/min. For 1.10 μm OMS (50 × 4.6 mm I.D.), the A/B = 80/20 (v/v), and the flow rate ranges from 0.2 to 2.4 mL/min. For the above separations, the column temperature was maintained at 35 °C, and the UV detector was set to 254 nm. The structure of the analyte used is listed in Table S6. the mobile phases included A (supercritical fluid CO_2) and B (methanol).

Test conditions for the retention behaviors: The BPR temperature and pressure were set to 60 °C and 150 bar, respectively. The mobile phases included mobile phases A (supercritical fluid CO_2) and B (methanol) at a flow rate of 3.0 mL/min. The column temperature was maintained at 35 °C, and the UV detector was set to 215 nm and 254 nm. Gradient elution was performed as follows: For retention mechanism: 0.0 min-15.0 min, 95%-65% (A). For retention characteristics: 0.0 min-10.0 min, 98%-60% (A). The structures of the analytes used are listed in Table S6.

Test conditions for weakly retained compounds: The BPR temperature was 60 ℃ and the pressure was 150 bar. The mobile phases included A (supercritical fluid CO_2) and B (methanol). The column temperature was maintained at 35 ℃ and the UV

detector was set at 210 nm. When separating unsaturated fatty acids, adopting isocratic elution, A/B = 99/1 (v/v), and the flow rate was 2.0 mL/min. When four tocopherol derivatives of vitamin E were separated, the gradient elution: 0.0 min-10.0 min, 99%-90% (A), 10.0 min-15.0 min, 90% (A) at a flow rate was 3.0 mL/min. When separating PLA, EPA, and DHA, neat supercritical CO_2 was used at a flow rate of 3.0 mL/min. The structures of the analytes used are listed in Table S6.

Test conditions for polar compounds: The BPR temperature was 60 ℃ and the pressure was 150 bar. The column temperature was maintained at 35℃, the UV detector was set at 254 nm and the flow rate was 3.0 mL/min. Comparison of retention strength: For OMS: Mobile phases were A (supercritical fluid CO_2) and B (methanol), A/B = 82/18 (v/v). While for silica gel: A/B = 90/10 (v/v). Separation of flavonoids: 0.0 min-10.0 min, 90%-65% (A). Separation of alkaloids: 0.0 min-10.0 min, 95%-65% (A). The structures of the analytes used are listed in Table S6.

Test conditions for Salvia miltiorrhiza Bunge: The BPR temperature was 60 ℃ and the pressure was 150 bar. When five standard compounds of *Salvia miltiorrhiza* Bunge were separated, the gradient elution was adopted. The mobile phases included A (supercritical fluid CO_2) and B (methanol). For other commercial columns: 0.0 min-10.0 min, 98%-65% (A) a flow rate was 3.0 mL/min, while for 2.33 μm OMS: 0.0 min-7.5 min, 85%-65% (A) at a flow rate was 3.0 mL/min, for 1.10 μm OMS: 0.0 min-7.5 min, 82%-65% (A) at a flow rate was 2.0 mL/min. When the extract of *Salvia miltiorrhiza* Bunge was separated, the gradient elution of OMS was 0.0 min-10.0 min, 98%-60% (A).

Supplementary figures

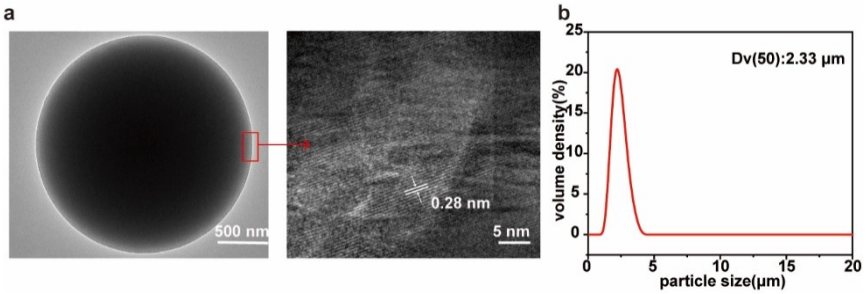

Figure S1. Characterization of 2.33 μm OMS particles. a) TEM micrograph. b) Particle size distribution measured by the dynamic light scattering.

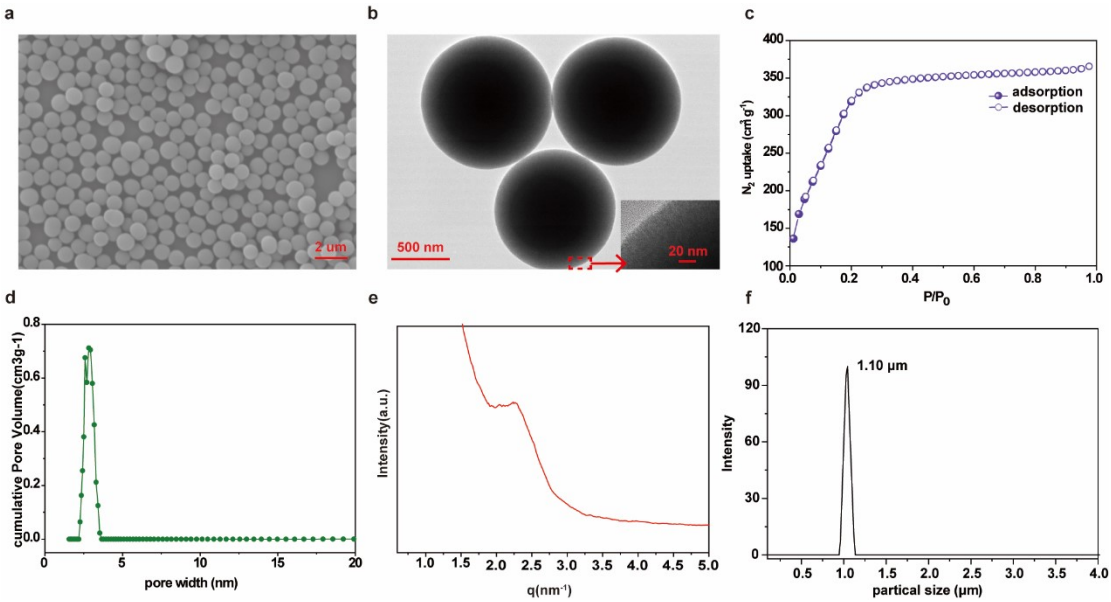

Figure S2. Characterization of 1.10 μm OMS particles. a) SEM micrograph. b) TEM micrograph. c) Nitrogen adsorption isotherms. d) Pore width calculated through NLDFT models. e) SAXS pattern. f) Particle size distribution measured by nanometer particle size potentiometer.

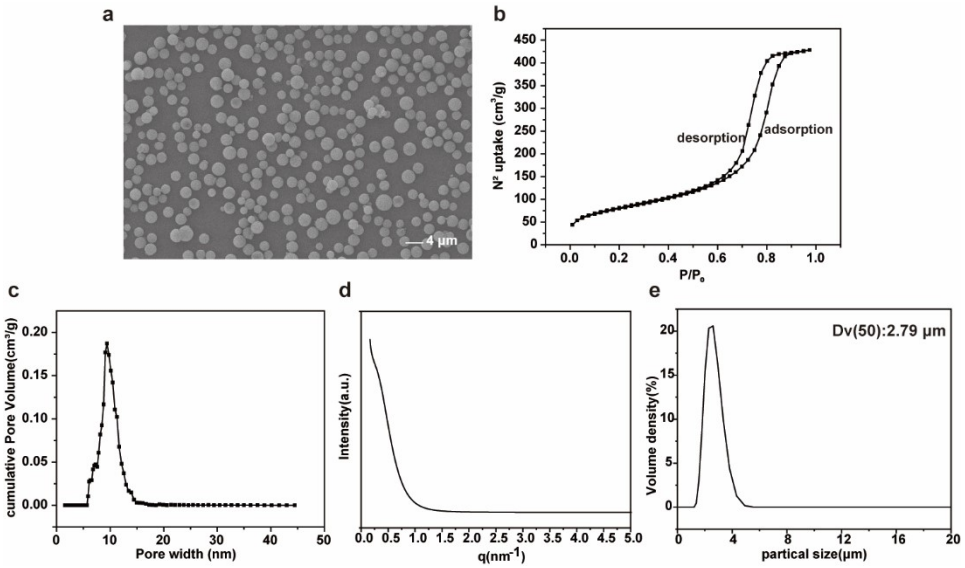

Figure S3. Characterization of conventional silica gel. a) SEM micrograph. b) Nitrogen adsorption isotherms. c) Pore width calculated through NLDFT models. d) SAXS pattern. e) Particle size distribution measured by the dynamic light scattering.

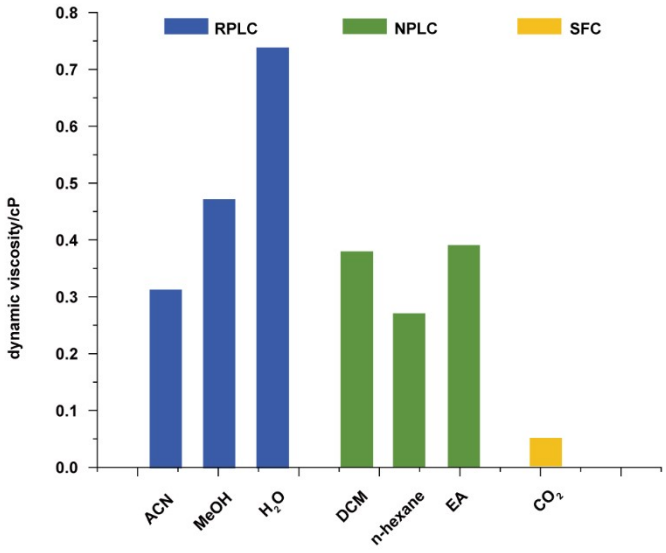

Figure S4. Comparison of the dynamic viscosity of the mobile phases used in different chromatographic modes. The test conditions: temperature is 35 °C and the pressure is 2000 psi (≈138 bar).

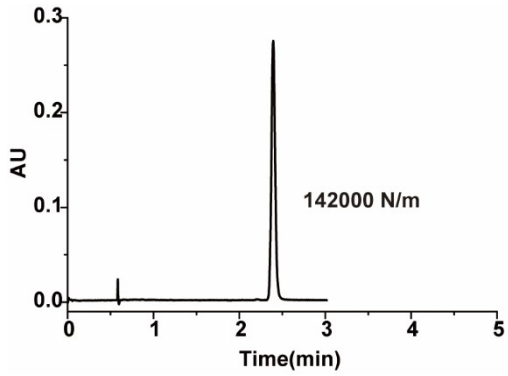

Figure S5. The chromatogram of optimal column efficiency for conventional silica gel. The chromatographic conditions: The BPR pressure was set to 2100 psi (≈145 bar), the mobile phases included A (supercritical fluid CO_2) and B (methanol). the A/B = 85/15 (v/v), and the flow rate is 1.5 mL/min. The column temperature was maintained at 35 °C, and the UV detector was set to 254 nm.

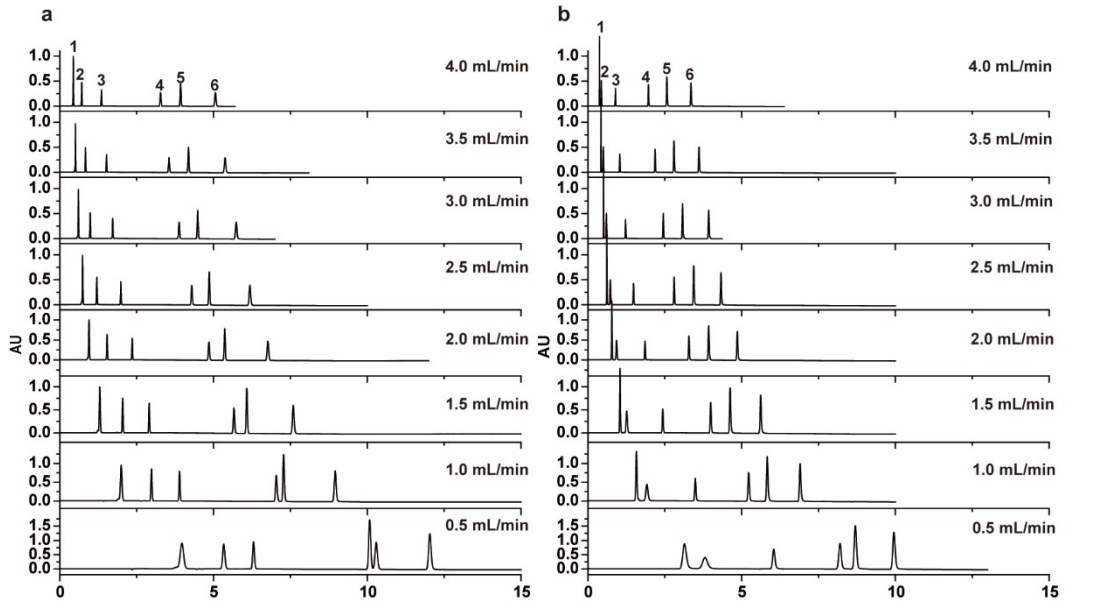

Figure S6. The chromatograms with common hydrophobic and hydrophilic analyte mixtures at different flow rates. a) The chromatograms of OMS. b) The chromatograms of conventional silica gel. The chromatographic conditions: The BPR pressure was set to 2100 psi (≈145 bar), the mobile phases included A (supercritical fluid CO_2) and B (methanol). The gradient elution: 0.0 min-10.0 min, 95%-65% (A) (v/v), and the flow rate ranges from 0.5 to 4.0 mL/min. The column temperature was maintained at 35 °C, and the UV detector was set to 215 nm. Peak 1: fluorene; Peak 2: benzoic acid; Peak 3: butyl p-hydroxybenzoate; Peak 4: thymine; Peak 5: phloroglucinol;

Peak 6: uridine.

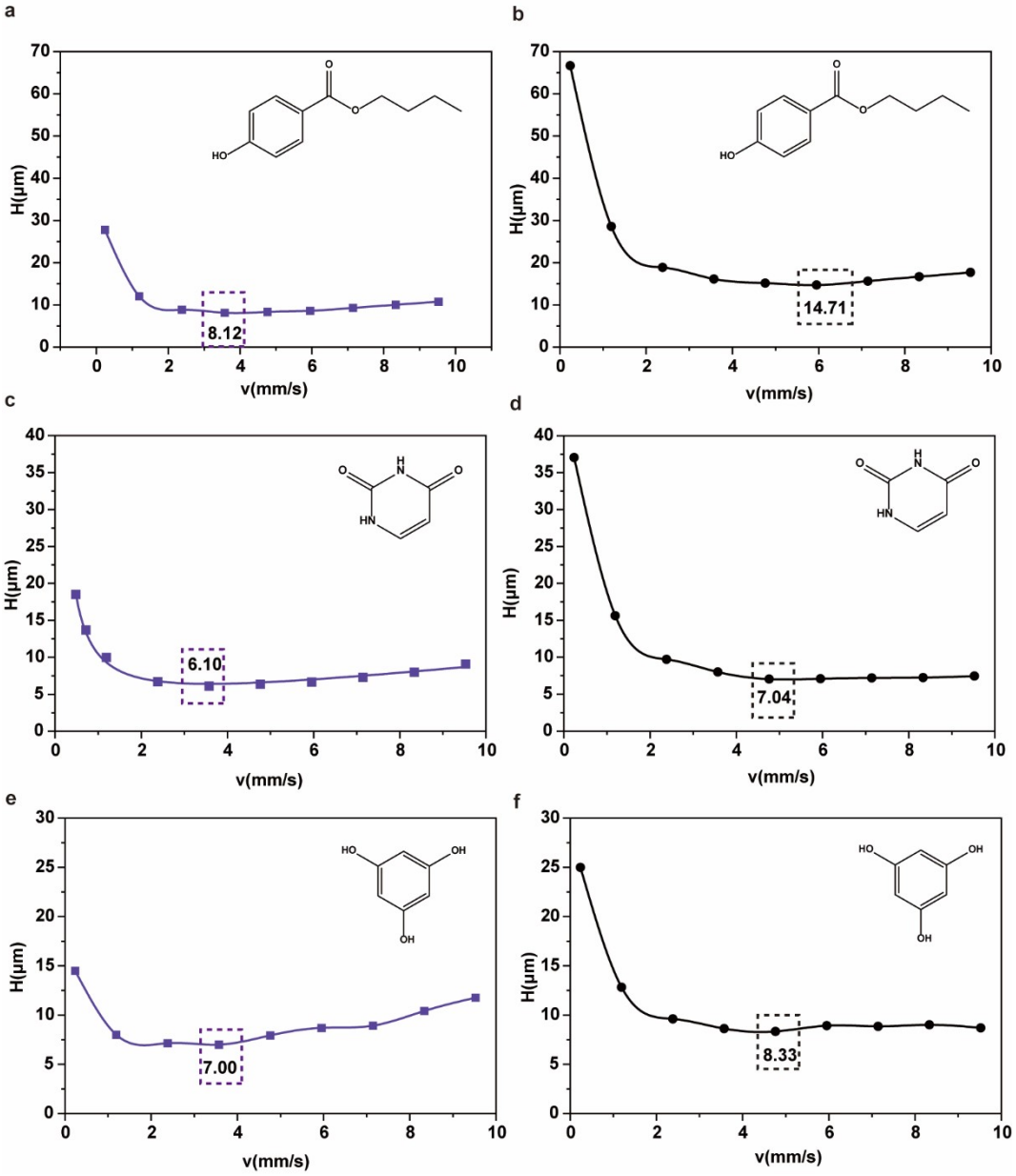

Figure S7. The Van-Deemter plots for different analytes. a, c, e) The results of OMS. b, d, f) The result of conventional silica gel. The chromatographic conditions: The BPR pressure was set to 2100 psi (≈145 bar), the mobile phases included A (supercritical fluid CO_2) and B (methanol). For butyl p-hydroxybenzoate, the A/B = 95/5 (v/v); For uracil, the A/B = 85/15 (v/v); For phloroglucinol, he A/B = 80/20 (v/v). The column temperature was maintained at 35 °C, and the UV detector was set to 215 nm.

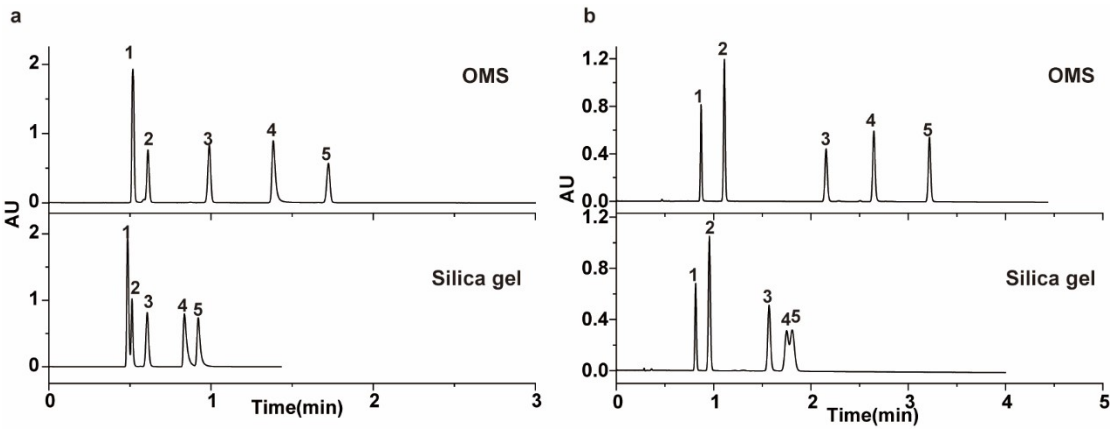

Figure S8. Chromatograms for separation of different analytes. a) Peak 1: naphthalene; Peak 2: fluorene; Peak 3: dimethyl phthalate; Peak 4: benzoic acid; Peak 5: aniline. b) Peak 1: coumarin; Peak 2: flavone; Peak 3: caffeine; Peak 4: thymine; Peak 5: prednisone. The chromatographic conditions: The BPR pressure was set to 2100 psi (≈145 bar), the mobile phases included A (supercritical fluid CO_2) and B (methanol). For a), the gradient elution: 0.0 min-5 min, 92%-95% (A) (v/v); For b), the gradient elution: 0.0 min-10 min, 95%-65% (A) (v/v); The column temperature was maintained at 35 °C, and the UV detector was set to 215 nm.

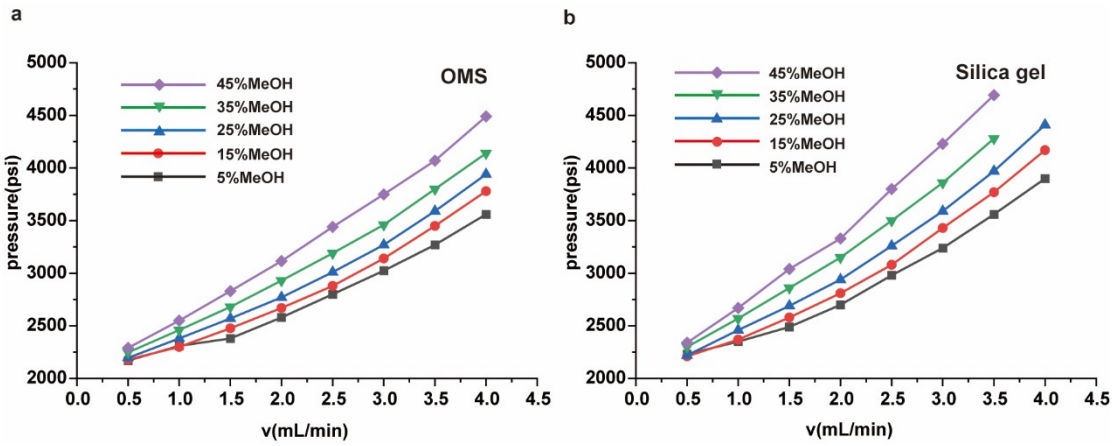

Figure S9. Comparison of back pressure/flow curves at different additive ratios. a) The results of OMS; b) The results of conventional silica. The chromatographic conditions: The BPR pressure was set to 2100 psi (≈145 bar), the mobile phases included A (supercritical fluid CO_2) and B (methanol). The purple line: 45%B (v/v); The green line: 35%B (v/v); The blue line: 25%B (v/v); The red line: 15%B (v/v); The black line: 5%B (v/v); The column temperature was maintained at 35 °C, and the UV detector was set to 215 nm.

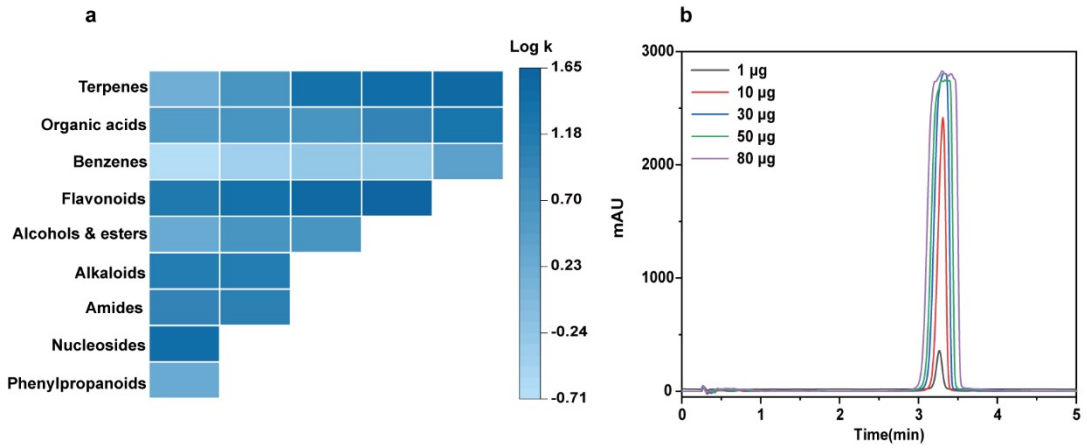

Figure S10. Retention mechanism of OMS in SFC. a) Heatmap of retention factors and compound types. b) Effect of injected analytes mass of etistradiol. The chromatographic conditions: The BPR pressure was set to 2100 psi (≈145 bar), the mobile phases included A (supercritical fluid CO_2) and B (methanol), the A/B = 85/15 (v/v). The column temperature was maintained at 35 °C, and the UV detector was set to 215 nm.

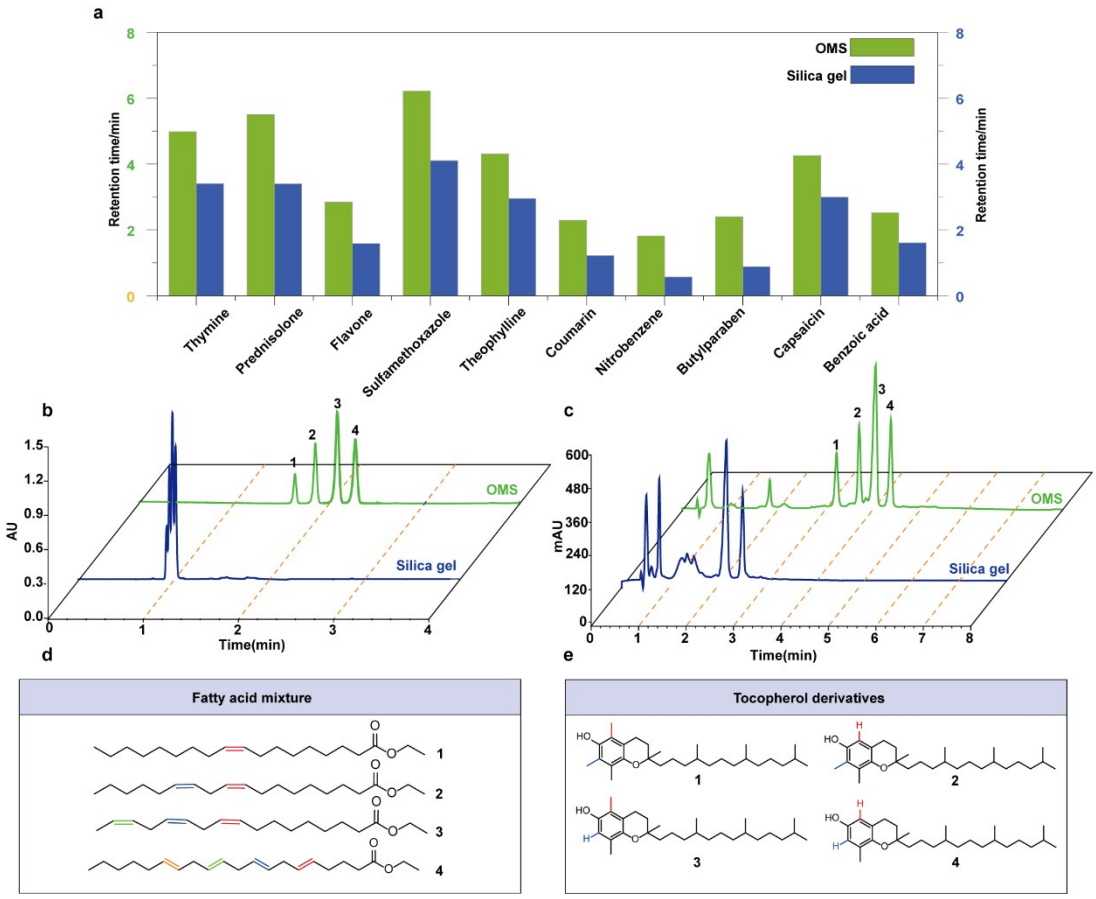

Figure S11. Retention characteristics of OMS during separation. a) The retention of different

compounds by OMS and silica gel was compared. b) Separation of unsaturated fatty acids. c) Separation of vitamin E derivatives. d) Structure diagram of unsaturated fatty acids. e) Structure diagram of vitamin E derivatives. The BPR temperature was 60 °C and the pressure was 150 bar. The mobile phases included A (supercritical fluid CO_2) and B (methanol). The column temperature was maintained at 35 °C and the UV detector was set at 210 nm. For a): the gradient elution: 0.0 min-10.0 min, 98%-60% (A) at a flow rate was 3.0 mL/min; For b), adopting isocratic elution, A/B = 99/1 (v/v), and the flow rate was 2.0 mL/min. For c), the gradient elution: 0.0 min-10.0 min, 99%-90% (A) at a flow rate was 3.0 mL/min.

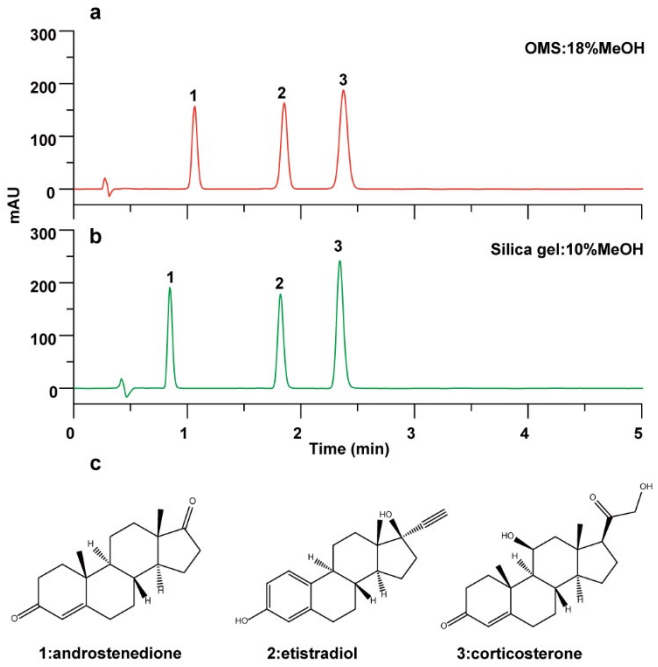

Figure S12. Comparison of elution strength. a) Retention of compounds on OMS. b) Retention of compounds on silica gel. c) Structure diagram. The BPR temperature was 60 °C and the pressure was 150 bar. The mobile phases included A (supercritical fluid CO_2) and B (methanol). The column temperature was maintained at 35 °C, the UV detector was set at 254 nm and the flow rate was 3.0 mL/min.

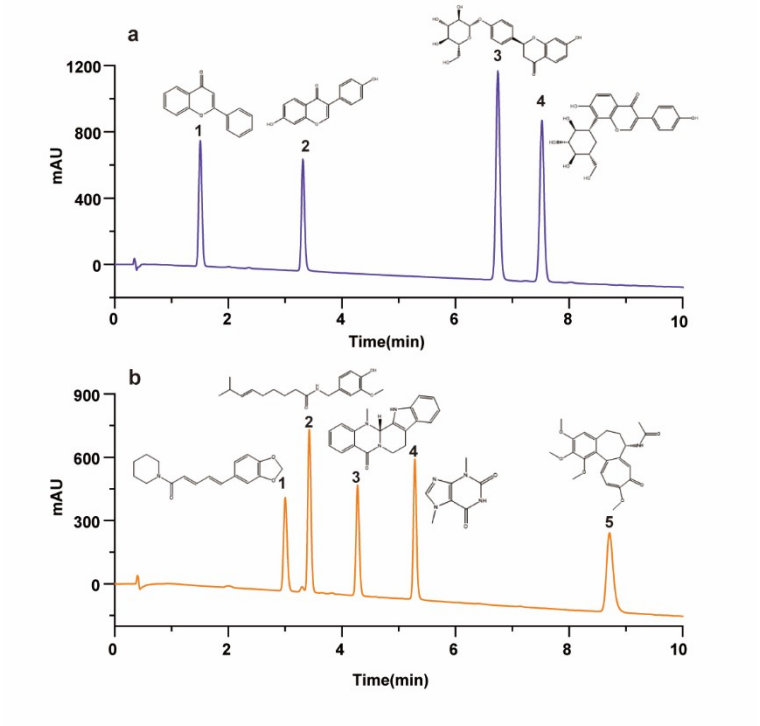

Figure S13. Separation of polar compounds on OMS. a) Separation results of flavonoids. b) Separation results of alkaloids. The BPR temperature was 60 °C and the pressure was 150 bar. The column temperature was maintained at 35 °C, the UV detector was set at 254 nm and the flow rate was 3.0 mL/min. For a): 0.0 min-10.0 min, 90%-65% (A). For b): 0.0 min-10.0 min, 95%-65% (A).

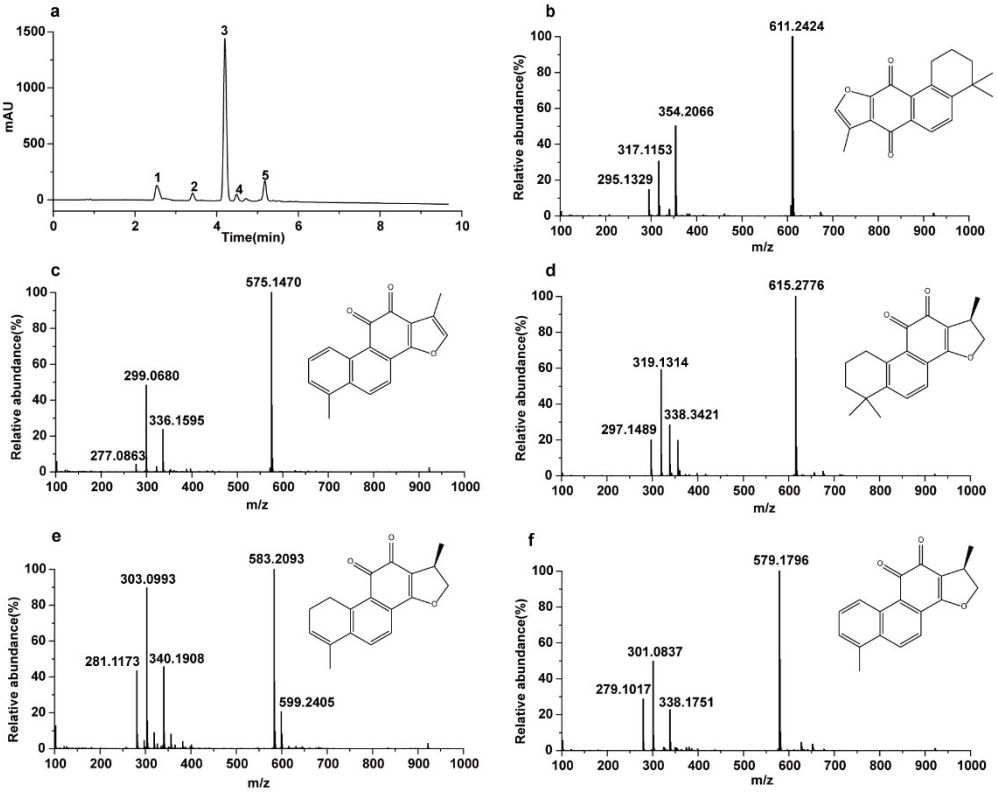

Figure S14. Separation and identification the extract of *Salvia miltiorrhiza* Bunge using SFC-MS. a) Separation of the extract by OMS. Mass spectrum of b) the first peak. c) the second peak. d) the third peak. e) the fourth peak. f) the fifth peak. The BPR temperature was 60 °C and the pressure was 150 bar. The mobile phases included A (supercritical fluid CO_2) and B (methanol). The gradient elution of OMS was 0.0 min-10.0 min, 98%-60% (A) at a flow rate of 3.0 mL/min.

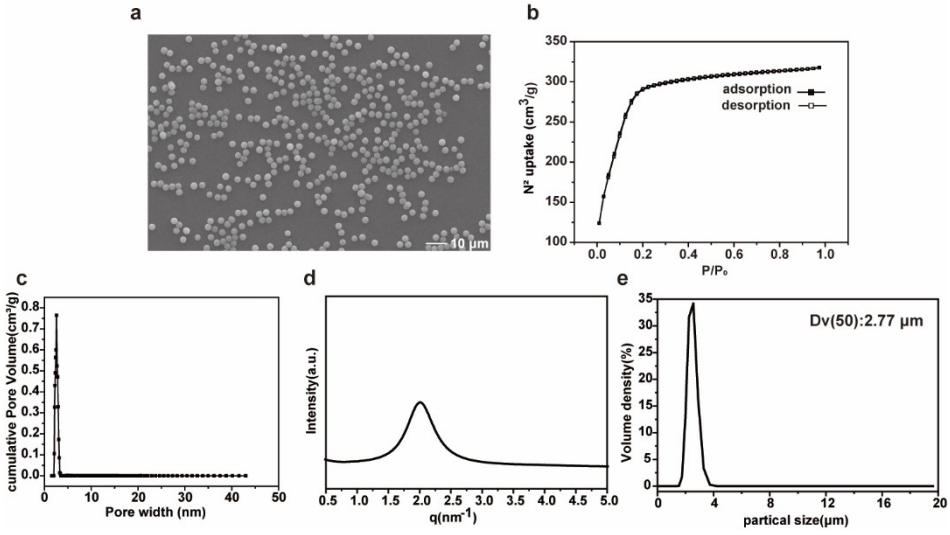

Figure S15. Characterization of OMS-SH. a) SEM micrograph. b) Nitrogen adsorption isotherms.

c) Pore width calculated through NLDFT models. d) SAXS pattern. e) Particle size distribution measured by the dynamic light scattering.

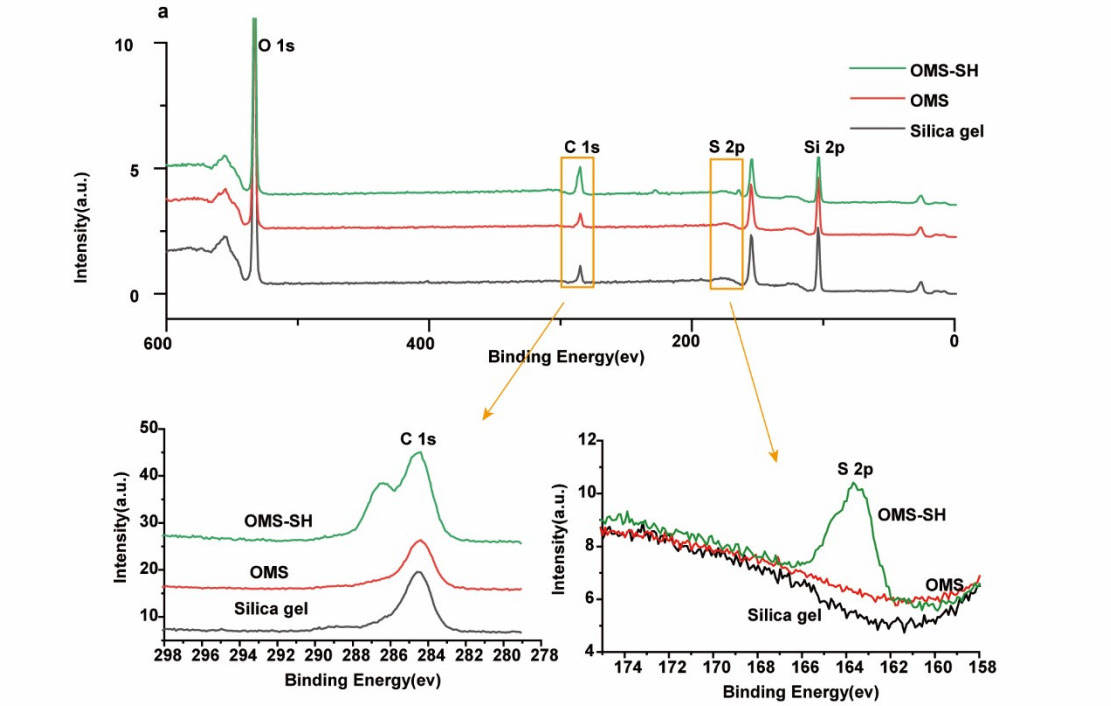

Figure S16. XPS spectrum of three materials.

Table S1. Particle size distribution and pore structure properties of particles

	surface area (m^2/g)	pore diameter (nm)	particle size (μm)	source
Silica gel	286	9.4	2.79	purchased from Fuji Silysia Chemical
2.33 μm OMS	1183	2.5	2.33	synthesis
1.10 μm OMS	1294	2.8	1.10	synthesis
OMS-SH	1149	2.6	2.77	synthesis

Table S2. Summary of structures and properties of analytes used in Figure 3.

	Compound name	Compound structure	CAS	M.V.	logP/ACD	Logk
No.1	Trimesitinic acid	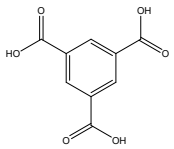	554-95-0	210.14	0.081±0.249	1.26
No.2	m-Phthalic acid	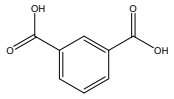	121-91-5	166.13	0.860±0.230	1.02

No.3	Benzeneformic acid	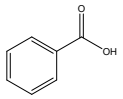	65-85-0	122.12	1.559±0.206	0.51
No.4	2-Naphthoic acid	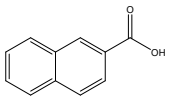	93-09-4	172.18	2.743±0.208	0.69
No.5	4-Biphenylacetic acid	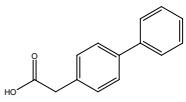	5728-52-9	212.24	3.260±0.256	0.69
No.6	Biphenyl	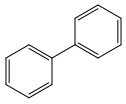	92-52-4	154.21	4.091±0.235	-0.29
No.7	1-Fluoronaphthalene	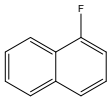	321-38-0	146.16	3.488±0.278	-0.31
No.8	Ethylbenzene	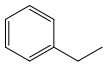	100-41-4	106.17	3.229±0.169	-0.71
No.9	Bromobenzene		108-86-1	157.01	2.936±0.277	-0.45
No.10	Nitrobenzene	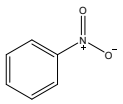	98-95-3	123.11	1.921±0.166	0.39
No.11	Benzyl alcohol	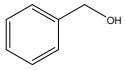	100-51-6	108.14	1.055±0.206	0.68
No.12	Uracil	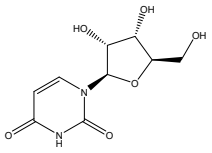	58-96-8	244.20	-1.581±0.321	1.46
No.13	p-Toluenesulfonamide	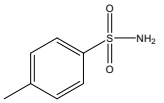	70-55-3	171.22	0.971±0.207	1.02
No.14	N-Benzylbenzenesulfonamide	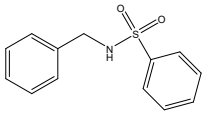	837-18-3	247.31	1.882±0.313	0.98
No.15	Dimethyl phthalate	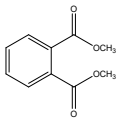	131-11-3	194.18	1.695±0.253	0.23
No.16	Butylparaben	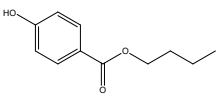	94-26-8	194.23	3.410±0.224	0.66
No.17	Eugenol	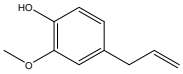	97-53-0	164.20	2.403±0.236	0.30

No.18	Andrographolid	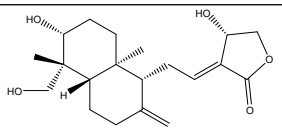	5508-58-7	350.45	0.424±0.430	1.42
No.19	Phytol	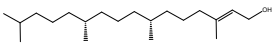	150-86-7	296.53	8.230±0.255	0.23
No.20	Antixerophthalmic vitamin	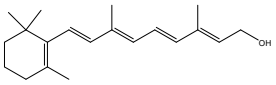	68-26-8	286.45	6.078±0.324	0.68
No.21	Kirenol	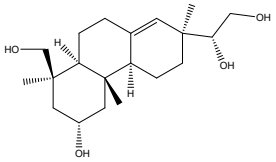	52659-56-0	338.48	1.900±0.381	1.56
No.22	Paclitaxel	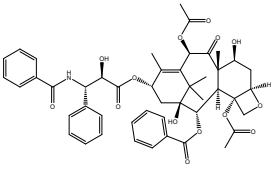	33069-62-4	853.91	3.950±0.808	1.41
No.23	Taxifolin	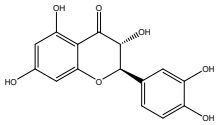	480-18-2	304.25	1.569±0.555	1.36
No.24	Baikalein	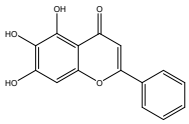	491-67-8	270.24	3.641±0.517	1.22
No.25	Liquiritoside	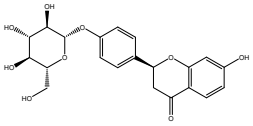	551-15-5	418.39	0.280±0.409	1.56
No.26	Puerarin	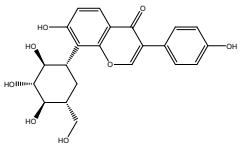	3681-99-0	416.38	0.408±1.243	1.65
No.27	Capsaicine	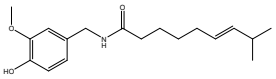	404-86-4	305.41	3.217±0.392	1.12
No.28	d-Evodiamine	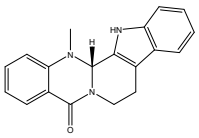	518-17-2	303.36	3.888±0.871	1.14

Table S3. Summarizing the chromatographic column used in this paper

	pore diameter (nm)	particle size (μm)	Column size	source	application
*2.33 μm OMS	2.5	2.33	4.6 mm*100 mm	synthesis	All tests in this paper except Van Deemter curve
*2.33 μm OMS	2.5	2.33	3 mm*100 mm	synthesis	Van Deemter curve
*1.10 μm OMS	2.8	1.10	4.6 mm*50 mm	synthesis	All tests in this paper
*Silica gel	9.4	2.79	4.6 mm*100 mm	purchased from Fuji Silysia Chemical	All tests in this paper except Van Deemter curve

*Silica gel	9.4	2.79	3 mm*100 mm	purchased from Fuji Silysia Chemical	Van Deemter curve
NH2	10	3.5	4.6 mm*100 mm	purchased from Acchrom	Separation of five principal compounds of Salvia miltiorrhiza Bge
Diol	10	3.5	4.6 mm*100 mm	purchased from Acchrom	Separation of five principal compounds of Salvia miltiorrhiza Bge
PIC	10	3.5	4.6 mm*150 mm	purchased from Waters	Separation of five principal compounds of Salvia miltiorrhiza Bge
*OMS-SH	2.6	2.77	4.6 mm*50 mm	synthesis	Separation of DHA, PLA and EPA by OMS-SH

*Column packing is done in our laboratory.

Table S4. Relative elemental surface composition by XPS for conventional silica, OMS, and OMS-SH

	C (%)	O (%)	Si (%)	S (%)
Silica gel	8.43	63.16	28.41	0
OMS	8.35	62.8	28.85	0
OMS-SH	18.6	55.8	24.12	1.48

Table S5. Elemental analysis results of OMS-SH

	N (%)	C (%)	H (%)	S (%)
OMS-SH	0.000	4.783	1.729	3.009

Table S6. Summary of detailed information of analytes used in the paper.

	Compound name	Compound structure	CAS	M.V.	manufacturer	Source
No.1	Uracil	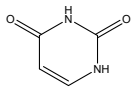	66-22-8	112.09	Macklin	Fig.2
No.2	Thymine	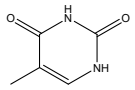	65-71-4	126.11	Macklin	Fig.S11a
No.3	Cortalone	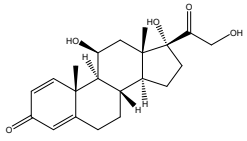	50-24-8	360.44	Sigma-Aldrich	Fig.S11a
No.4	Flavone	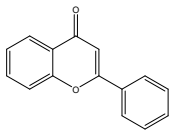	525-82-6	222.24	Macklin	Fig.S11a

No.5	Sulphamethoxazole	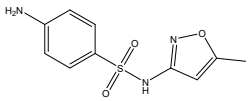	723-46-6	253.28	Sigma-Aldrich	Fig.S11a
No.6	Theophylline	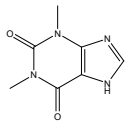	58-55-9	180.16	Macklin	Fig.S11a
No.7	Coumarin	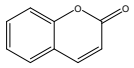	91-64-5	146.14	Acros	Fig.S11a
No.8	Nitrobenzene	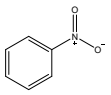	98-95-3	123.11	Macklin	Fig.S11a
No.9	Dimethyl phthalate	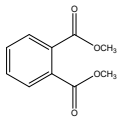	131-11-3	194.18	Macklin	Fig.S11a
No.10	Capsaicine	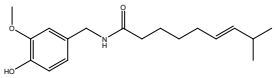	404-86-4	305.41	Macklin	Fig.S11a
No.11	2-Naphthoic acid	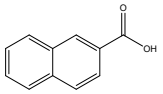	93-09-4	172.18	Macklin	Fig.S11a
No.12	Ethyl oleate	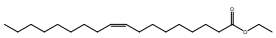	111-62-6	310.52	J&K Scientific	Fig.S11b
No.13	Ethyl linoleate	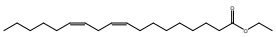	544-35-4	308.50	J&K Scientific	Fig.S11b
No.14	Ethyl linolenoate	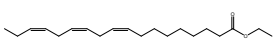	1191-41-9	306.48	J&K Scientific	Fig.S11b
No.15	Ethyl arachidonate	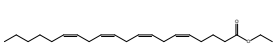	1808-26-0	332.52	J&K Scientific	Fig.S11b
No.16	(±)-α-Tocopherol	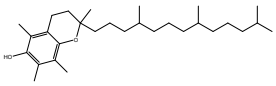	10191-41-0	430.71	prepared in our laboratory	Fig.S11c
No.17	β-Tocopherol	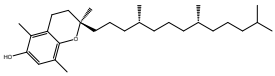	148-03-8	416.68	prepared in our laboratory	Fig.S11c
No.18	γ-Tocopherol	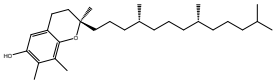	54-28-4	416.68	prepared in our laboratory	Fig.S11c
No.19	δ-Tocopherol	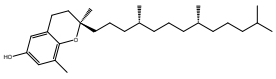	119-13-1	402.65	prepared in our laboratory	Fig.S11c
No.20	Methyl tanshinonate	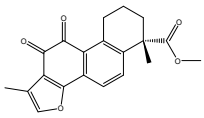	18887-19-9	338.35	the National Institutes for Food and Drug Control	Fig.4
No.21	Tanshinone I	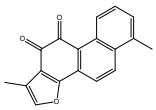	568-73-0	276.29	the National Institutes for Food and Drug Control	Fig.4

No.22	Tashinone IIA	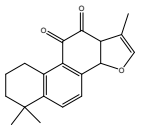	568-72-9	294.35	the National Institutes for Food and Drug Control	Fig.4
No.23	Danshenol A	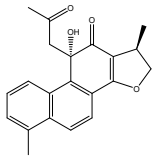	189308-08-5	336.38	the National Institutes for Food and Drug Control	Fig.4
No.24	Dihydrotanshinone I	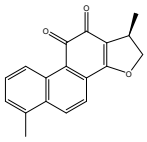	87205-99-0	278.30	the National Institutes for Food and Drug Control	Fig.4
No.25	Methyl palmitelaidate	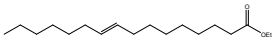	10030-74-7	268.44	J&K Scientific	Fig.5
No.26	5,8,11,14,17-Eicosapentaenoic acid, ethyl ester	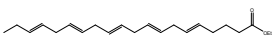	84494-70-2	330.50	J&K Scientific	Fig.5
No.27	4,7,10,13,16,19-Docosahexaenoic acid, ethyl ester	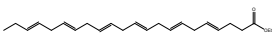	84494-72-4	356.54	J&K Scientific	Fig.5
No.28	Etistradiol	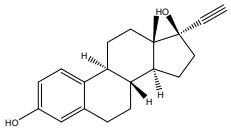	57-63-6	296.40	Acros	Fig.S10b &Fig.S12
No.29	Fluorene	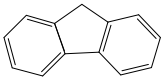	86-73-7	166.22	Macklin	Fig.S6& Fig.S8a
No.30	Benzoic acid	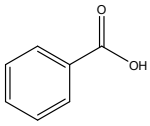	65-85-0	122.12	Macklin	Fig.S6& Fig.S8a
No.31	Butyl p-hydroxybenzoate	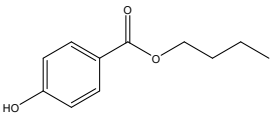	94-26-8	194.23	Macklin	Fig.S6
No.32	Thymine	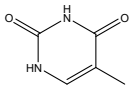	65-71-4	126.11	Macklin	Fig.S6& Fig.S8b
No.33	Phloroglucinol	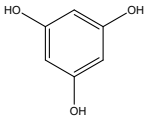	108-73-6	126.11	Acros	Fig.S6
No.34	Uridine	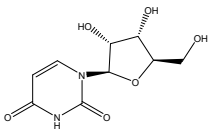	58-96-8	244.20	Macklin	Fig.S6
No.35	naphthalene	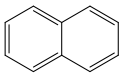	91-20-3	128.17	Macklin	Fig.S8a

No.36	dimethyl phthalate	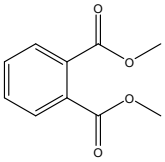	131-11-3	194.18	Macklin	Fig.S8a
No.37	aniline	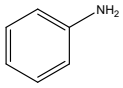	62-53-3	93.13	Macklin	Fig.S8a
No.38	coumarin	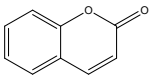	91-64-5	146.14	Acros	Fig.S8b
No.39	caffeine	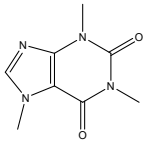	58-08-2	194.19	Macklin	Fig.S8b
No.40	prednisone	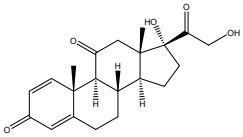	53-03-2	358.43	Acros	Fig.S8b
No.~~29~~ 41	Androstenedione	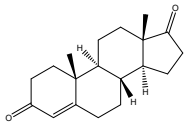	63-05-8	286.41	Acros	Fig.S12
No.42	Corticosterone	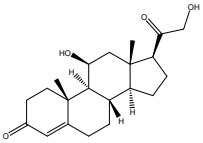	50-22-6	346.46	Acros	Fig.S12
No.43	Piperine	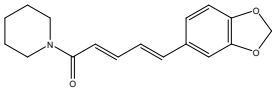	94-62-2	285.34	the National Institutes for Food and Drug Control	Fig.S13
No.44	Capsaicine	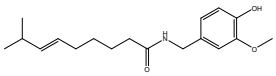	404-86-4	305.41	Macklin	Fig.S13
No.45	Evodiamine	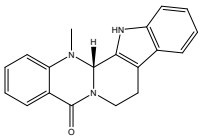	518-17-2	303.36	Macklin	Fig.S13
No.46	Theobromine	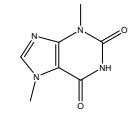	83-67-0	180.16	Macklin	Fig.S13
No.47	Colchicine	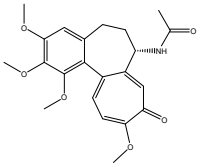	64-86-8	399.44	J&K Scientific	Fig.S13
No.48	Flavone	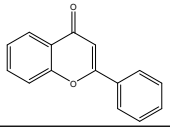	525-82-6	222.24	Macklin	Fig.S13 & Fig.S8b

No.49	Daidzein	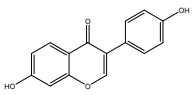	486-66-8	254.24	Merck	Fig.S13
No.50	Liquiritoside	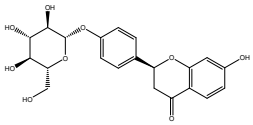	551-15-5	418.39	Macklin	Fig.S13
No.51	Puerarin	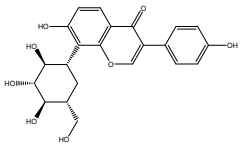	3681-99-0	416.38	Macklin	Fig.S13

J&K Scientific (Beijing, China); Merck (Darmstadt, Germany); Macklin (Shanghai, China); the National Institutes for Food and Drug Control (Beijing, China); Acros (Fair Lawn, NJ, USA); Sigma-Aldrich (St. Loius, MO, USA).

references

1. L. P. Cheng, J. F. Cai and Y. X. Ke, *Journal of Inorganic and Organometallic Polymers and Materials*, 2019, **29**, 1417-1421.